

Published in final edited form as:

Naunyn Schmiedebergs Arch Pharmacol. 2009 May ; 379(5): 453–460. doi:10.1007/s00210-008-0385-5.

Actions of kurtoxin on tetrodotoxin-sensitive voltage-gated Na⁺ currents, Na_v1.6, in murine vas deferens myocytes

Hai-Lei Zhu,

Department of Pharmacology, Graduate School of Medical Sciences, Kyushu University, 3-1-1 Maidashi, Higashi Ward, Fukuoka 812-8582, Japan

Richard D. Wassall,

Department of Pharmacology, University of Oxford, Mansfield Road, Oxford OX1 3QT, UK

Thomas C. Cunnane, and

Department of Pharmacology, University of Oxford, Mansfield Road, Oxford OX1 3QT, UK

Noriyoshi Teramoto

Department of Pharmacology, Graduate School of Medical Sciences, Kyushu University, 3-1-1 Maidashi, Higashi Ward, Fukuoka 812-8582, Japan

Abstract

Kurtoxin is described as a selective inhibitor of Ca_v3.1. Using patch-clamp techniques, the modulatory effects of kurtoxin on tetrodotoxin-sensitive voltage-gated Na⁺ currents (*I*_{Na}) recorded from mouse vas deferens myocytes were investigated. Kurtoxin increased the peak amplitude of *I*_{Na} between -40 and -30 mV, whilst inhibited the peak amplitude at more positive potentials than -10 mV, thereby demonstrating a dual action on the peak amplitude of *I*_{Na}. The time to reach the peak amplitude of *I*_{Na} became significantly longer in the presence of kurtoxin in comparison with that of the controls. Kurtoxin also slowed the deactivation of *I*_{Na} at more positive membrane potentials than -30 mV. Kurtoxin enhanced the total amount of electrical charge of *I*_{Na} in a concentration-dependent manner. These results suggest that kurtoxin is a modulator of Na_v1.6 in native freshly dispersed smooth muscle cells from mouse vas deferens as well as its action on Ca_v3.1.

Keywords

Kurtoxin; Smooth muscle; Sodium currents; Vas deferens

Introduction

Kurtoxin, a toxic peptide of 63 amino acids isolated from the venomous scorpion, *Parabuthus transvaalicus*, inhibits low-threshold voltage-dependent T-type Ca²⁺ channels (i.e. Ca_v3.1) expressed in *Xenopus* oocytes with relatively high potency and high selectivity. The toxin has been described as a promising tool for functional and structural studies of low-threshold Ca_v and was used as a valuable peptide for defining the involvement of these Ca_v in electrical and biochemical signalling (Chuang et al. 1998). However, at higher concentrations, kurtoxin also inhibits the peak currents due to high-

threshold Ca_V (i.e. L-type and N-type Ca^{2+} channels; Ca_V1 family and $\text{Ca}_V2.2$, respectively) and facilitates P-type Ca^{2+} channel currents ($\text{Ca}_V2.1$) in isolated neurons (Sidach and Mintz 2002). Furthermore, kurtoxin accelerates the deactivation of T-type and L-type Ca^{2+} currents, slows the deactivation of P-type Ca^{2+} currents and does not affect N-type Ca^{2+} current kinetics (Sidach and Mintz 2002). Conversely, using expression systems to study voltage-gated Na^+ channel (Na_V) function, kurtoxin caused a slowing of inactivation of Na_V in cloned $\text{IIA}\alpha$ subunits co-expressed with β_1 subunits (Chuang et al. 1998) and in cloned, cardiac-like hH1 Na^+ channels (Olamendi-Portugal et al. 2002) expressed in *Xenopus* oocytes. However, the effects of kurtoxin on Na^+ channel currents (I_{Na}) have not been previously characterised in native cells or smooth muscle-type Na_V (i.e. $\text{Na}_V1.6$). Since it is generally believed that electrophysiological and pharmacological properties of I_{Na} differ from molecular types of Na_V (Catterall et al. 2005), it is important to investigate the effects of kurtoxin on smooth muscle-type Na_V ($\text{Na}_V1.6$). Given that the channel kinetics of $\text{Ca}_V3.1$ are also similar to those of Na_V (such as transient activation, fast decay of current inactivation, low-threshold for activation etc.) in smooth muscle cells, it is essential to have selective pharmacological tools to distinguish electrophysiological properties between $\text{Ca}_V3.1$ and Na_V , which may be expressed in the same cells.

Recently, we reported the biophysical and molecular properties of a tetrodotoxin (TTX)-sensitive I_{Na} recorded from mouse vas deferens freshly dispersed smooth muscle cells, demonstrating that the molecular identity of Na_V in these smooth muscle cells is mainly $\text{Na}_V1.6$, which is encoded by the *Scn8a* gene (Zhu et al. 2008). To characterise the kurtoxin selectivity on I_{Na} in native cells, it would seem that this dispersed smooth muscle cell system would be exceptionally useful, as mouse vas deferens smooth muscle cells lack expression of other TTX-sensitive Na_V and TTX-resistant Na_V . Additionally, I_{Na} are absent in knockout mice for $\text{Na}_V1.6$ [motor end-plate disease (med) mouse, $\text{Na}_V1.6^{-/-}$] (Kohrman et al. 1996), meaning that the sole contributor to functional currents in these cells is $\text{Na}_V1.6$ (Zhu et al. 2008). Taken together, these results suggest that dispersed cells from the mouse vas deferens are an attractive system to investigate the effects of kurtoxin on I_{Na} , as any result can be attributed to action at the specific channel, $\text{Na}_V1.6$.

Although there were similarities between the expression systems for $\text{Na}_V1.6$ and the present results from native cells, there were also some striking differences (channel kinetics, IC_{50} value for TTX; see Zhu et al. 2008). Firstly, we found that kurtoxin possesses not only inhibitory effects on the peak amplitude of I_{Na} but also that peak I_{Na} is increased at some membrane potentials (a dual action on the peak amplitude of I_{Na}). Secondly, we compared different concentrations of kurtoxin to investigate any action on channel kinetics of Na_V , showing a slowing of I_{Na} activation and deactivation after toxin application. Finally, we found that kurtoxin enhanced the total amount of electrical charge moving due to I_{Na} . These unique properties make kurtoxin an asset for structural studies of channel gating in smooth muscle-type Na_V (i.e. $\text{Na}_V1.6$) and also show the different effects that kurtoxin has in native versus expression systems, providing important evidence validating the use of murine vas deferens cells as an assay system for $\text{Na}_V1.6$.

Materials and methods

Cell dispersion

Male BALB/c mice (8-10 weeks) were killed by cervical dislocation, and vasa deferentia were removed and placed immediately in physiological salt solution (PSS, see below). All experiments were approved by the Animal Care and Use Committee of the Faculty of Medicine, Kyushu University. Efforts were made to minimise the use of animals; several types of experiment were carried out on aliquots of cells from an animal. Mouse vas deferens single smooth muscle cells were isolated freshly by the gentle tapping method

(described previously in Teramoto and Brading 1996) and stored at 4°C. After isolation, relaxed spindle-shaped cells were stored on ice-cold PSS and used within 3-4h.

Recording procedure

Patch-clamp experiments (conventional whole-cell configuration) were performed at room temperature (21-23°C) and the data recording system used was essentially the same as that described previously (Teramoto et al. 2005). The whole-cell current data were filtered at 1-5 kHz by an eight-pole Bessel filter (Multifunction Filter 3611, NF Corporation, Yokohama, Japan) sampled at 100 μs and analysed on a PowerMac G4 computer (Apple Computer Japan, Tokyo, Japan) using Chart v5.0.2 (ADInstruments, Castle Hill, Australia). The mean peak amplitude of I_{Na} (the nearest five points before and after the peak values, i.e. within 1 ms duration around the peak value) was not significantly different between 1 and 5 kHz, suggesting that the filtering process did not miss any fast events, i.e. the representation after filtering was not different from the values sampled without filtering (see Heinemann 1995). Similar results were obtained from 20 other cells. As a consequence, the current traces in the figures were obtained from records filtered at 1 kHz for analysis and presentation in order to avoid continuous signals becoming indistinguishable during sampling (i.e. aliasing) and to reduce background noise.

Steady-state inactivation of the current was assessed using a two-step protocol in which the cells were stepped from -70 mV to a range of voltages between -120 and +40 mV for a period of 2 s before a 200 ms step to -10 mV. The peak amplitude of I_{Na} evoked by each test pulse was measured. The peak amplitude of I_{Na} without application of any conditioning pulse was normalised as one. The lines were drawn by fitting the data to the Boltzmann's equation by the least-squares method:

$$I = (I_{max}) / \{1 + \exp[(V - V_{half})/k]\}$$

where I , I_{max} , V , V_{half} and k are the relative amplitude of I_{Na} observed at various amplitudes of the conditioning pulse (I) and observed with application of the conditioning pulse of -70 mV (I_{max}), the amplitude of the conditioning pulse (V), and where the amplitude of I_{Na} was reduced to half (V_{half}) and the slope factor (k), respectively. The steady-state inactivation curves in the absence or presence of kurtoxin were drawn using the values given in the figure legend (see Fig. 1d).

Activation curves were derived from the current-voltage relationships, and conductance (G) was calculated from the equation:

$$G = I_{Na} / (E_m - E_{Na})$$

where I_{Na} is the peak current elicited by depolarising test pulses from -60 to +30 mV from the holding membrane potential (E_m) of -70 mV and E_{Na} is the equilibrium potential for Na^+ . E_{Na} was estimated from current-voltage relationship curves where the extrapolated line, fitted with the current-voltage relationship curve, crossed over the zero line (Hille 1992). G_{max} is the maximal Na^+ conductance (calculated at potentials above +10 mV). The G/G_{max} ratios were plotted against the membrane potential as relative amplitudes. In Fig. 3d, activation curves were obtained from the current-voltage relationships of Fig. 3b, fitting to the Boltzmann's equation.

The integrated area (2 s duration) of the transient I_{Na} (pC; total amount of charge) was measured in the absence and presence of kurtoxin. The curve for kurtoxin was drawn by fitting the equation using the least-squares method:

$$\text{Relative amplitude of } I_{Na} = 1 + 1 / \{1 + (EC_{50}/D)^{n_H}\}$$

where EC_{50} , D and n_H are the dissociation constant, concentration of kurtoxin (nM) and Hill's coefficient, respectively.

Solutions and drugs

The composition of the bath solution (i.e. PSS) was (in mM): 140 NaCl, 5 KCl, 1.2 MgCl₂, 2 CaCl₂, 5 glucose, 10 HEPES (pH 7.35-7.40 with Tris base). The composition of the pipette solution was (mM): 130 CsCl, 10 tetraethylammonium (TEACl), 2 MgCl₂, 5 glucose, 5 EGTA, 5 ATP, 10 HEPES (pH 7.35-7.40 with Tris base). Cells were allowed to settle in the small experimental chamber (80 μ l in volume) which was superfused by gravity throughout the experiments at a rate of 2 ml/min from a solution reservoir. TTX (Sankyo, Tokyo, Japan) and kurtoxin (Peptide Institute, Osaka, Japan) were dissolved in deionised water. All other drugs were purchased from Sigma-Aldrich (Sigma-Aldrich Japan K.K., Tokyo, Japan).

Data analysis

Statistical comparisons were performed using Student's *t* test for paired observations, taking $P < 0.05$ as significant. Changes were considered significant at $P < 0.05$. Data are expressed as mean with the standard deviation (SD).

Results

Effects of kurtoxin on voltage-gated Na⁺ currents in native mouse vas deferens myocytes

In a conventional whole-cell configuration, at potentials more positive than -40 mV, a fast transient inward current was evoked and reached a peak, which then decayed gradually in the presence of 100 μ M Cd²⁺ (Fig. 1a, b). The transient inward current was suppressed reversibly by application of 1 μ M TTX in the vas deferens myocytes [i.e. they were TTX-sensitive voltage-gated Na⁺ currents (I_{Na}); as described previously in Zhu et al. 2008]. The peak amplitude of I_{Na} was maintained for at least 20 min when test depolarisation pulses were applied at 20 s intervals (the peak amplitude of transient inward current at 20 min being 98% of the value determined after reaching steady state; $n=37$ cells, from 12 different animals). Consequently, all experiments were performed within a 20 min period in the presence of 100 μ M Cd²⁺ in order to investigate the effects of kurtoxin on I_{Na} .

As shown in Fig. 1b, the maximum peak amplitude was obtained at approximately -10 mV, and the amplitude was reduced at more positive potentials, demonstrating a voltage dependency. In the presence of 500 nM kurtoxin, the peak amplitude of I_{Na} was enhanced at -40 and -30 mV ($P < 0.05$; see Fig. 1c). In contrast, at more positive potentials than -10 mV, kurtoxin inhibited the peak amplitude of I_{Na} ($P < 0.05$; see Fig. 1c). However, apart from its dual effects on peak I_{Na} amplitude, kurtoxin also produced a pronounced slowing in both time-to-peak of the current amplitude and current decay. In order to investigate further the effects of kurtoxin on inactivation and activation at different voltages in I_{Na} , inactivation and activation curves were obtained, as shown in Fig. 1d. The voltage-dependent inactivation was investigated before and after application of kurtoxin using the experimental protocol (conditioning pulse duration was 2 s; holding membrane potential was -70 mV). In the absence of kurtoxin (control), inactivation of I_{Na} occurred with conditioning pulses

positive to -70 mV. In the presence of kurtoxin (approximately 5 min later), the voltage-dependent inactivation curve in the same cells was not shifted significantly (see Fig. 1d). The 50% inactivation potentials, evaluated by means of Boltzmann fitting, were -48.0 ± 4.5 mV for controls ($n=7$ cells, three different animals) and -49.8 ± 5.4 mV for cells in the presence of kurtoxin ($n=7$ cells, three different animals), respectively ($P>0.05$). The activation curves obtained from the current-voltage relationships in the absence and presence of 500 nM kurtoxin, fitted to the Boltzmann equation, are also shown in Fig. 1d. Kurtoxin caused no significant shift of the activation curves; the 50% activation potentials were -23.5 ± 3.2 mV in controls ($n=6$ cells, four different animals) and -25.1 ± 3.4 mV in the presence of kurtoxin ($n=6$ cells, four different animals; $P>0.05$).

The time difference between when I_{Na} was elicited by rectangular voltage pulses and when I_{Na} reached the maximum value was measured in the absence and presence of 500 nM kurtoxin (Fig. 2a-c). In the presence of kurtoxin, the time to reach the peak amplitude of I_{Na} was slowed significantly between -30 and 0 mV (Fig. 2d). Kurtoxin slowed the time to reach the peak amplitude of I_{Na} in comparison with control when the depolarising pulse was applied from a holding membrane potential of -70 to -10 mV (Fig. 2e), demonstrating a concentration dependence.

The time constant of the current decay of I_{Na} was measured from when the rectangular pulse (a depolarising pulse of 2 s to -10 mV from a holding potential of -70 mV) was applied (Fig. 3a). I_{Na} evoked by this long duration depolarising pulse declined with a single time constant (1.4 ± 0.1 ms, $n=6$ cells, from five different animals). The decay time constant of I_{Na} to several membrane potentials (from -30 to +20 mV) was estimated by a single exponential as shown in Fig. 3b. The time constant of the current decay became faster in a voltage-dependent manner. When 500 nM kurtoxin was applied, the peak amplitude of I_{Na} was inhibited and the decay of I_{Na} was slowed (Fig. 3a). In the presence of kurtoxin, I_{Na} evoked by a long depolarising pulse declined with two different time constants (fast component, $\tau_f=6.3 \pm 1.1$ ms, $n=6$ cells, five different animals; slow component, $\tau_s=191.6 \pm 50.6$ ms, $n=6$ cells, five different animals). Similarly, the time constant of I_{Na} decay to several membrane potentials (from -30 to +20 mV) was fitted by double exponentials and became smaller in a voltage-dependent manner (Fig. 3b). As shown in Fig. 3c, the integrated area of I_{Na} (2 s duration) from the baseline was also calculated as the total amount of the electrical charge in the absence and presence of 500 nM kurtoxin, demonstrating a bell-shaped relation. In the presence of kurtoxin, the integrated area of I_{Na} increased significantly in comparison to that of control. Figure 3d summarised the relative value of the integrated area of I_{Na} at all membrane potentials tested from -30 to +20 mV when the integrated area of I_{Na} in control was normalised as one at each membrane potential. In Fig. 3e, kurtoxin (10 nM-1 μ M) enhanced the integrated area of I_{Na} (2 s duration, -10 mV) from the baseline in a concentration-dependent manner ($EC_{50}=365.1$ nM).

Discussion

This study demonstrates how kurtoxin affects I_{Na} in freshly dispersed smooth muscle cells, consistent with its inhibition of cloned I_{Na} studied previously in *Xenopus* oocytes [neuronal-like Na^+ channels (Chuang et al. 1998) and cardiac-like hH1 Na^+ channels (Olamendi-Portugal et al. 2002)]. To our knowledge, this is the first example of kurtoxin producing a dual effect of increasing and decreasing the peak values of I_{Na} by modifying the gating of TTX-sensitive Na_V in native cells and enhancing the total amount of the electrical charge in a concentration-dependent manner.

Biophysical actions of kurtoxin on I_{Na}

Kurtoxin shares 30-60% sequence homology with other α -scorpion Na_V toxins, so it is perhaps not surprising that kurtoxin has effects on Na_V (see Chuang et al. 1998). Kurtoxin probably mediates its effects through changing the gating properties of Na_V , as the time delay between the applied depolarising pulse and the peak amplitude of I_{Na} was slowed compared to controls (inhibition of Na^+ channel opening) and, conversely, kurtoxin caused a slower inactivation of I_{Na} (inhibition of Na^+ channel closing).

We have demonstrated here that application of kurtoxin produced a pronounced slowing of both activation and inactivation of I_{Na} (composed of $Na_V1.6$ in mouse vas deferens smooth muscle cells, see Zhu et al. 2008) compared to I_{Na} in the absence of kurtoxin (control). These were similar to the results described for the cloned rat brain II α subunits co-expressed with β_1 subunits (Chuang et al. 1998). However, we also found that kurtoxin enhanced the total electrical charge moved in I_{Na} evoked by depolarising step pulses between -30 and +20 mV and, as a result, suggests that kurtoxin binds to α subunits of $Na_V1.6$, modifying channel gating, and enhances the total electrical charge in I_{Na} .

It has been reported that kurtoxin inhibited the peak amplitude of $Na_V1.5$ channel currents expressed in *Xenopus* oocytes at -30 mV and that kurtoxin caused no effect on the peak amplitude of $Na_V1.5$ channel currents at more positive potentials than -20 mV when the membrane potential was held at -90 mV (Olamendi-Portugal et al. 2002). In contrast, in mouse vas deferens freshly dispersed myocytes (i.e. native cells), kurtoxin increased significantly the peak amplitude of I_{Na} at -30 mV and decreased the peak amplitude of I_{Na} at more positive potentials than -20 mV, showing a dual action on the peak amplitude of I_{Na} when the membrane potential was held at -70 mV. It is not certain whether or not these different channel kinetics may vary due to the different types of α subunit channel proteins ($Na_V1.2$ vs. $Na_V1.6$) or experimental conditions (membrane potentials, native cells versus *Xenopus* oocyte expression systems, concentration of kurtoxin, the lack of β subunits modifying the channel function as an auxiliary subunit etc.). It is well known that electrophysiological and pharmacological properties of $Na_V1.X$ differ from their molecular types of α subunits (Catterall et al. 2005). For example, TTX-sensitive and TTX-insensitive Na^+ channels have been identified in a single family of $Na_V1.X$. Moreover, even in TTX-sensitive Na^+ channels (such as $Na_V1.1$, $Na_V1.2$, $Na_V1.3$, $Na_V1.4$, $Na_V1.6$ and $Na_V1.7$), different potency of TTX was also observed, depending on molecular types of $Na_V1.X$ (Catterall et al. 2005). Thus, it is generally thought that the effects of the compounds (toxins, blockers, activators etc.) on the activity of $Na_V1.X$ might be tested in each type of $Na_V1.X$. In the present experiments, we have been able to demonstrate the dual action of kurtoxin on the $Na_V1.6$ currents in native smooth muscle myocytes. Moreover, in the presence of kurtoxin, the current inactivation also changed from a single exponential in control to a double exponential, although the precise mechanism behind this is unclear. The simple explanation is that kurtoxin induced the activation of other types of Na_V : in mouse portal vein for example, Saleh et al. (2005) reported the presence of multiple types of Na_V (i.e. $Na_V1.6$ and $Na_V1.7$). However, Zhu et al. (2008) show that the only contributor to functional Na^+ currents in mouse vas deferens smooth muscle cells is $Na_V1.6$ using $Na_V1.6$ -null mice (med mouse, $Na_V1.6^{-/-}$), so although kurtoxin-induced activation of other types of Na_V in mouse vas deferens smooth muscle cells is a possibility, it seems unlikely. In contrast, it has been reported that Na^+ channel blockers prevent channel closure, shifting a gating equilibrium of the channel (Yamamoto 1986; Yeh and Narahashi 1977). In the presence of kurtoxin, the time to reach the peak amplitude of I_{Na} and the current decay of I_{Na} are decelerated in a voltage- and concentration-dependent manner. Thus, kurtoxin may modify the channel kinetics of $Na_V1.6$ in mouse vas deferens myocytes, shifting the voltage sensitivity of the gating mechanisms in the pore regions. Even with the decreased peak amplitude of I_{Na} at higher voltages, kurtoxin increased significantly the total amount of I_{Na}

evoked by depolarising rectangular pulses (i.e. the amount of electrical charge) in comparison to that in control. These results suggest that kurtoxin may modify Na_V opening kinetics from a short- to a long-opening mode, allowing more Na^+ influx into the cells, and may behave differently in native smooth muscle cells compared to *Xenopus* oocyte expression systems.

Is kurtoxin a selective T-type Ca^{2+} channel blocker?

Kurtoxin inhibits α_{1G} T-type Ca^{2+} channel currents in a concentration-dependent manner ($K_d=15$ nM; Chuang et al. 1998). At 350 nM, kurtoxin suppressed the α_{1G} T-type Ca^{2+} channel currents and inhibited the α_{1H} T-type Ca^{2+} channel currents (closely related to α_{1G}) by about 85% (Chuang et al. 1998). This suggests that kurtoxin binds to α_{1H} with nearly as high an affinity as α_{1G} . In contrast, the same concentration of kurtoxin (350 nM) did not affect α_{1A} , α_{1B} , α_{1C} or α_{1E} , suggesting that the K_d of kurtoxin binding to these channels is probably greater than 10 μM . These results show that kurtoxin can distinguish between α_{1G} and the high Ca_V with over 600-fold selectivity (Chuang et al. 1998).

In the present experiments, we have demonstrated that kurtoxin (100 nM) had little effect on the peak amplitude of I_{Na} and that kurtoxin (300 nM) inhibited the peak amplitude of I_{Na} at -10 mV. These concentrations are approximately tenfold higher than concentrations which are specific for T-type Ca^{2+} channels. In general, many channel blockers seem to be non-specific if used at high enough concentrations. However, we have demonstrated that kurtoxin caused an enhancement of the peak amplitude of I_{Na} at more negative potentials than -30 mV. These results suggest that kurtoxin possesses a specific effect on I_{Na} in native cells. Furthermore, as kurtoxin enhanced the total amount of the electrical charge in I_{Na} ($\text{EC}_{50}=365.1$ nM), taken together, these results suggest that kurtoxin is likely to be a modulator of $\text{Na}_V1.6$.

In conclusion, given that kurtoxin can affect a wide range of Ca_V , it is not appropriate to define kurtoxin as a selective T-type Ca^{2+} channel blocker, particularly at concentrations 300 nM where it affects Na^+ currents in native smooth muscle cells. As Na_V are often expressed in systems where Ca_V may also be expressed, care should be taken when using kurtoxin as a pharmacological tool to dissect Na_V and Ca_V present in the system. Although the importance of the present study is to show the toxin to be of limited value as a specific probe for studying ion channels, due to the dual action on $\text{Na}_V1.6$, kurtoxin may yet prove to be an important modulator of $\text{Na}_V1.6$ activation and inactivation, refining further our models of $\text{Na}_V1.6$ behaviour.

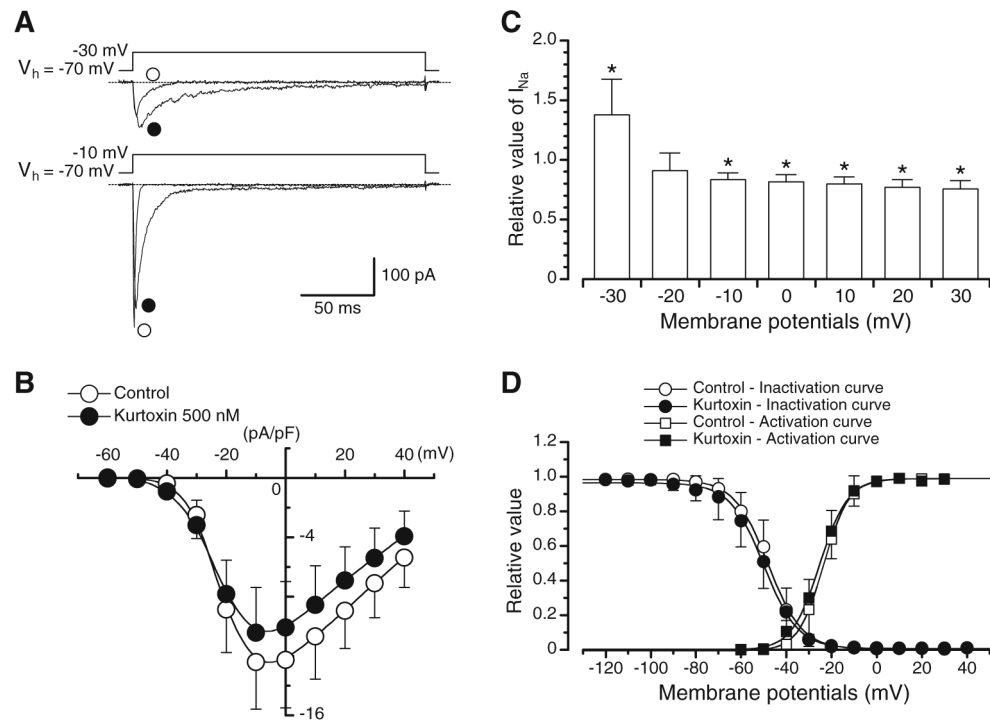
Acknowledgments

This work was supported by a Grant-in-Aid for Exploratory Research from the Japanese Society for the Promotion of Science (19650733 to Noriyoshi Teramoto), a Grant-in-Aid for Scientific Research (B) from the Japanese Society for the Promotion of Science (20300178 to Noriyoshi Teramoto) and a Grant-in-Aid from the Japan Science and Technology Agency (Noriyoshi Teramoto, Grant Number 15-B01-2008). This work was also supported by the Goho Life Sciences International Fund (2008 to Noriyoshi Teramoto). Dr Hai-Lei Zhu was awarded by a Grant-in-Aid from the Japan Society for the Promotion of Science (FY2007 JSPS Postdoctoral Fellowship for Foreign Researcher, P 07196 to Noriyoshi Teramoto). Dr Thomas C. Cunnane is supported by the Wellcome Trust (069768) and Mr. Richard D. Wassall is a British Pharmacological Society A.J. Clark Student.

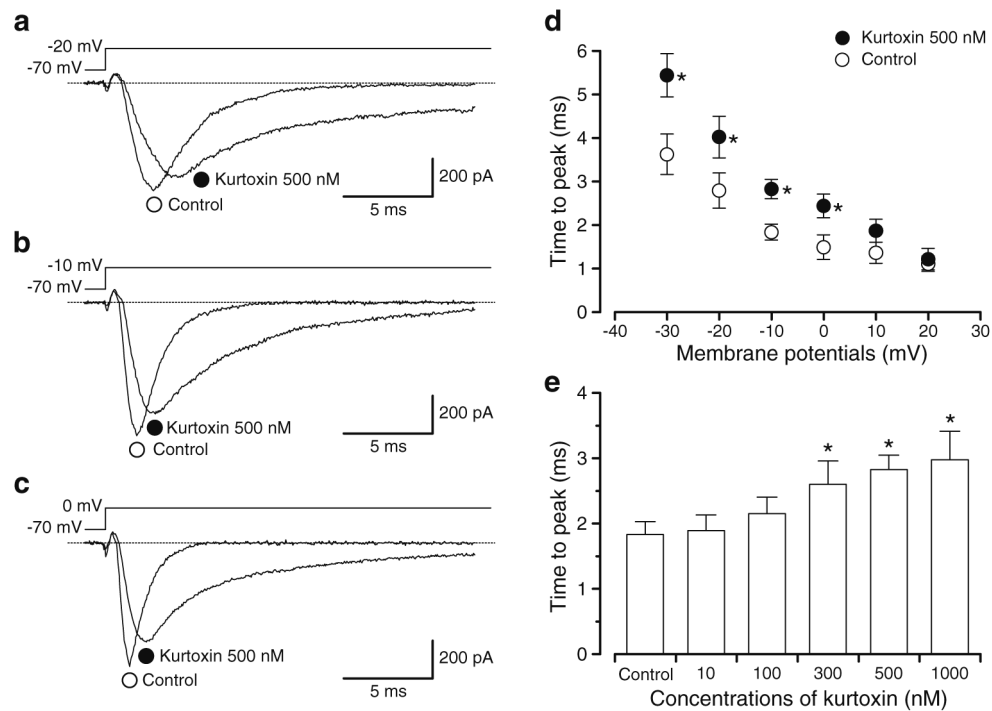
References

- Catterall WA, Goldin AL, Waxman SG. International union of pharmacology. XLVII. Nomenclature and structure-function relationships of voltage-gated sodium channels. *Pharmacol Rev.* 2005; 57:397–409. [PubMed: 16382098]
- Chuang RS, Jaffe H, Cribbs L, Perez-Reyes E, Swartz KJ. Inhibition of T-type voltage-gated calcium channels by a new scorpion toxin. *Nat Neurosci.* 1998; 1:668–674. [PubMed: 10196582]

- Heinemann, SH. Guide to data acquisition and analysis. In: Sakmann, B.; Neher, E., editors. Single-channel recording. 2nd edn.. Plenum; New York: 1995. p. 53-91.
- Hille, B. Selective permeability: independence. In: Hille, B., editor. Ionic channels of excitable membranes. 2nd edn.. Sinauer; Massachusetts: 1992. p. 337-361.
- Kohrman DC, Harris JB, Meisler MH. Mutation detection in the med and medJ alleles of the sodium channel *Scn8a*. Unusual splicing due to a minor class AT-AC intron. J Biol Chem. 1996; 271:17576–17581. [PubMed: 8663325]
- Olamendi-Portugal T, Garcia BI, Lopez-Gonzalez I, Van Der Walt J, Dyason K, Ulens C, Tytgat J, Felix R, Darszon A, Possani LD. Two new scorpion toxins that target voltage-gated Ca²⁺ and Na⁺ channels. Biochem Biophys Res Commun. 2002; 299:562–568. [PubMed: 12459175]
- Saleh S, Yeung SY, Prestwich S, Pucovsky V, Greenwood I. Electrophysiological and molecular identification of voltage-gated sodium channels in murine vascular myocytes. J Physiol. 2005; 568:155–169. [PubMed: 16020462]
- Sidach SS, Mintz IM. Kurtoxin, a gating modifier of neuronal high- and low-threshold Ca²⁺ channels. J Neurosci. 2002; 22:2023–2034. [PubMed: 11896142]
- Teramoto N, Brading AF. Activation by levcromakalim and metabolic inhibition of glibenclamide-sensitive K channels in smooth muscle cells of pig proximal urethra. Br J Pharmacol. 1996; 118:635–642. [PubMed: 8762088]
- Teramoto N, Tomoda T, Ito Y. Mefenamic acid as a novel activator of L-type voltage-dependent Ca²⁺ channels in smooth muscle cells from pig proximal urethra. Br J Pharmacol. 2005; 144:919–925. [PubMed: 15723098]
- Yamamoto D. Dynamics of strychnine block of single sodium channels in bovine chromaffin cells. J Physiol. 1986; 370:395–407. [PubMed: 2420978]
- Yeh JZ, Narahashi T. Kinetic analysis of pancuronium interaction with sodium channels in squid axon membranes. J Gen Physiol. 1977; 69:293–323. [PubMed: 845593]
- Zhu HL, Aishima M, Morinaga H, Wassall RD, Shibata A, Iwasa K, Nomura M, Nagao M, Sueishi K, Cunnane TC, Teramoto N. Molecular and biophysical properties of voltage-gated Na⁺ channels in murine vas deferens. Biophys J. 2008; 94:3340–3351. [PubMed: 18192366]

**Fig. 1.**

Actions of kurtoxin on I_{Na} . **a** Original current traces before and after application of kurtoxin at -30 and -10 mV. **b** Current-voltage relationships obtained in the absence or presence of kurtoxin. The current amplitude was measured as the peak amplitude of I_{Na} at each membrane potential. Each point indicates the current density (pA/pF), showing the mean +SD ($n=7$ cells, five different animals) shown by vertical lines. Some of the SD bars are less than the size of the symbol. **c** Relationship between the test potential and the relative value of I_{Na} in the presence of kurtoxin. The peak amplitude of I_{Na} evoked by depolarising pulses of various amplitudes in the absence of kurtoxin was normalised as one. Each column indicates the mean+SD ($n=7$ cells, five different animals) shown by vertical lines. Asterisks indicate a statistically significant difference demonstrated using a paired t test ($P<0.05$). **d** Effects of kurtoxin on the voltage-dependent activation and inactivation curves of I_{Na} . Steady-state inactivation curves, obtained in the absence and presence of kurtoxin, were fitted to the Boltzmann's equation using the following values: control, $V_{half}=-48.0$ mV and $k=7.5$; kurtoxin, $V_{half}=-49.8$ mV and $k=7.5$. Each symbol indicates the mean+SD shown by vertical lines ($n=7$ cells, three different animals; $P>0.05$). Some of the SD bars are less than the size of the symbol. Activation curves in the absence and presence of kurtoxin, fitting to the Boltzmann's equation using the following values: control, $V_{half}=-23.5$ mV and $k=6.0$; kurtoxin, $V_{half}=-25.1$ mV and $k=6.0$. Each symbol indicates the mean+SD shown by vertical lines ($n=6$ cells, four different animals; $P>0.05$).

**Fig. 2.**

Modulation of current upstroke in I_{Na} by kurtoxin. **a-c** The current trace of I_{Na} in the absence and presence of kurtoxin at the indicated membrane potential (**a** -20 mV, **b** -10 mV and **c** 0 mV) from -70 mV. **d** The time to reach the peak amplitude of I_{Na} was measured from when the depolarising pulse was applied. Each *symbol* indicates the mean \pm SD shown by *vertical lines* ($n=7$ cells, four different animals). *Asterisk* indicates a statistically significant difference and changes were considered significant at $P<0.05$ (using a paired t test). **e** Kurtoxin (10 nM-1 μ M) prolonged the time to reach the peak amplitude of I_{Na} in a concentration-dependent manner at -10 mV from -70 mV. *Asterisks* indicate a statistically significant difference demonstrated using a paired t test ($P<0.05$)

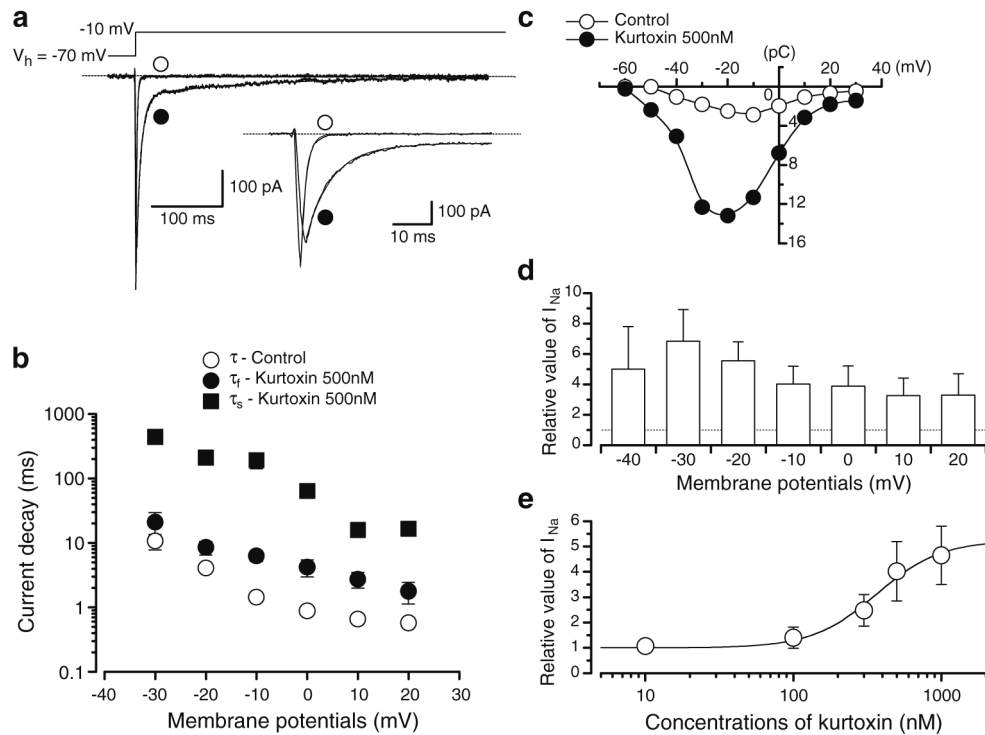


Fig. 3.

Modulation of I_{Na} by kurtoxin. **a** The current traces of I_{Na} in the absence and presence of kurtoxin. Both current traces were superimposed. *Inset traces*, expanded traces of the initial 50 ms duration elicited by rectangular voltage pulses. In the absence of kurtoxin, the current decay of I_{Na} was well fitted by a single exponential ($\tau=1.4\pm 0.1$ ms, $n=6$ cells, five different animals). In the presence of kurtoxin, I_{Na} declined with two different time constants (fast component, $\tau_f=6.3\pm 1.1$ ms, $n=6$ cells, five different animals; slow component, $\tau_s=191.6\pm 50.6$ ms, $n=6$ cells, five different animals). **b** The time constant of the current decay in the absence and presence of kurtoxin was summarised. The time constant was obtained from exponential fits of the decaying phase of I_{Na} at different potentials as listed. Each *symbol* indicates mean \pm SD shown by *vertical lines*. Some of the SD bars are smaller than the *symbols*. **c** Charge (pC)-voltage (mV) relationships obtained in the absence and presence of kurtoxin. **d** Relative value of the peak amplitude of I_{Na} enhanced by kurtoxin, expressed as a fraction of the electrical charge evoked by various amplitudes of depolarising pulses (2 s duration) in the absence of kurtoxin. Each *symbol* indicates mean \pm SD shown by *vertical lines* ($n=5$ cells, four different animals). *Asterisks* indicate a statistically significant difference demonstrated using a paired *t* test ($P<0.05$). **e** Relationship between the relative enhancement of total electric charge in I_{Na} and the concentration of kurtoxin (10 nM-1 μ M). The fraction of the electrical charge evoked by depolarising pulses from -70 to -10 mV (2 s duration) in the absence of kurtoxin was normalised as 1.0. The curve for kurtoxin was drawn by fitting the equation using the following values: $EC_{50}=365.1$ nM, $n_H=2.0$. Each *symbol* indicates the mean of 18 observations (12 different animals) with \pm SD shown by *vertical bars*.